Supplementary Information

High Pressure Cell for Edge Jumping X-ray Absorption Spectroscopy: Applications to industrial liquid sulfidation of hydrotreatment catalysts

Lesage, C.[1,2]; Devers, E.[1]; Legens, C.[1]; Fernandes[1], G.; Roudenko, O,[2], Briois, V.[2]

[1] *IFP Energies nouvelles, Rond-point de l'échangeur de Solaize BP3, 69360 Solaize*
[2] *Synchrotron SOLEIL L'orme des Merisiers, 91192 Gif-sur-Yvette Cedex, France*

Corresponding authors: clement.lesage@ifpen.fr and christele.legens@ifpen.fr

1. Suppliers

- Reactor tubes:
  Glassy carbon rods with an outer diameter of 4.7 mm: Hochtemperatur-Werkstoffe GmbH (HTW), http://www.htw-germany.com/
  Drilling of the rods: Micro-mécanique-Expert en precision, https://micro-mecanique.fr/
- Graphite/Vespel ferules: Restek VG2 60% vespel / 40% graphite 1/4 to 3/16 reducing (Ref: 20258), http://www.restek.fr/
- Thermocouple ferule: Vulcanic Ferule of 1.57 mm (REF= 4000607 according to Vulcanic scheme n°835402) drilled at 1 mm supplied by Vulcanic, http://www.vulcanic.com/fr/
- Gas/liquid distribution system was provided by Swagelock, https://www.swagelok.com.fr/fr-FR
- All the remaining items were custom made by Lucchese s.a.s, http://www.lucchese.fr/

2. Safety review

Main risks towards liquid sulfidation of an HDS catalyst are fire due to the presence of H_2, poisoning by H_2S and blast of the reactor due to the pressure. Below are presented the solutions to control these risks.

- Fire: The unit is put under nitrogen to avoid any contact of hydrogen with oxygen. A leak test is performed at the experiment pressure plus 15% leading to 35 bar for an experiment at 30 bar. After this first validation, the pressure is set at 30 bar, nitrogen is replaced by hydrogen and a second leak test is performed using a hydrogen leak detector.
- Poisoning by H_2S: Leak detection prevents any leak of H_2S. The exhaust gases are collected into the dangerous gases network of the synchrotron facilities.
- Blast of the reactor: To perform a high pressure reaction, it is required for the tube to sustain twice the operating pressure. In this case, the tubes were tested at 60 bar to enable a reaction at 30 bar. As the evolution of reactor towards pressure is still unknown, each reactor can only be used once.
- Electrical shortcut of the oven: alumina or quartz insert are used to centre the glassy carbon tube in the oven to avoid any contact of the oven with the tube.

3. Comparison of the EXAFS signal from the gas and the liquid sulfidation cell at the Co K edge

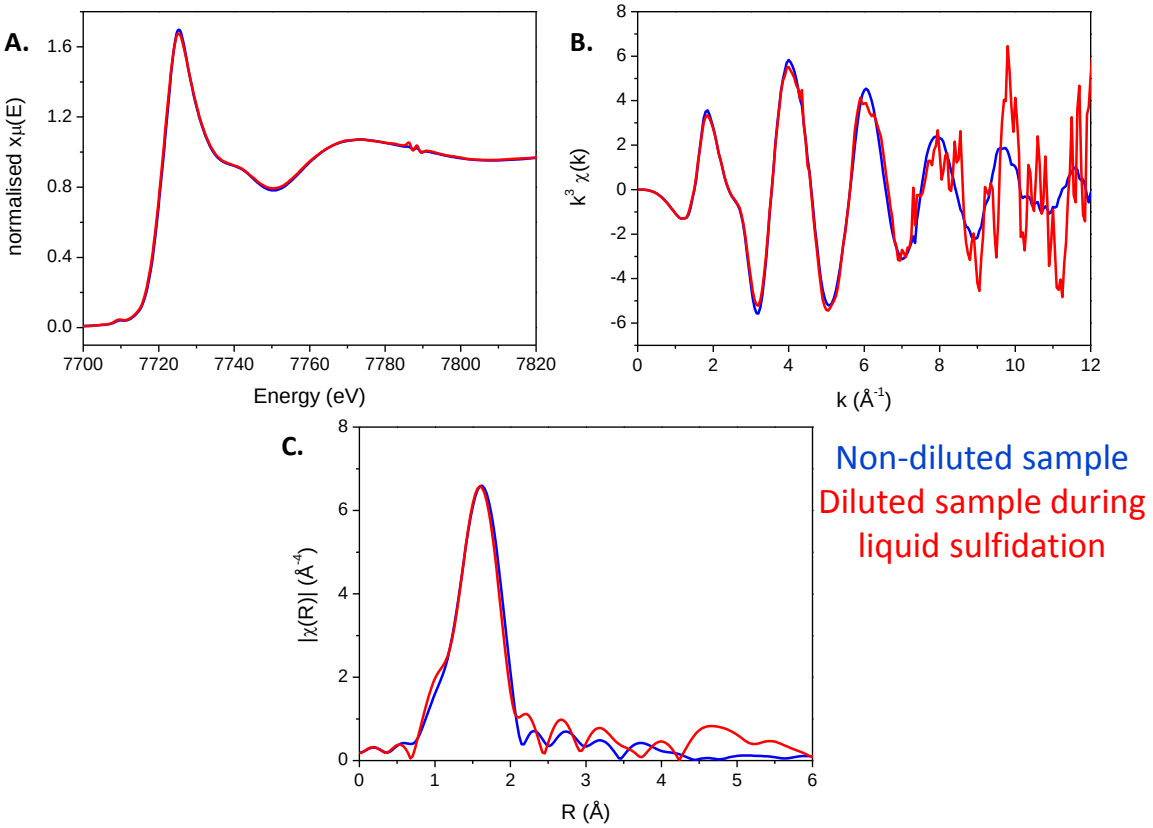

Figure S1 Comparison of the XAS signal (A.), the EXAFS signal (B.) and Fourier Transforms (FT) (C) between 2.4 to 8.3 $Å^{-1}$ measured at the Co K edge of a dried CoMoP catalyst at room temperature for the pure sample loaded in a thin quartz capillary (blue curves) and for the diluted sample loaded in the liquid sulfidation cell (red curves).

4. Extraction and Normalization interface

Two user-friendly graphical interfaces have been developed at the ROCK beamline by Olga Roudenko to handle the high number of data collected at very high frame rate. The first one, called *extract_gui* (Figure S2), is used in order to transform the binary nexus files recorded every 5s by the 16-bit analog to digital converter and scalar card containing the ionization chambers currents and the position of the angular encoder into ASCII files containing 10 columns with Energy (1), Bragg Angle (2), absorbance for the sample (3), absorbance for the reference foil (4), signal of the ionization chambers (I_0, I_1 and I_2) (5 to 7), monochromator direction (8), fluorescence signal (9) and time from start (10). The *extract_gui* allows to interpolate the raw energy values associated to each spectrum into a common extraction energy grid necessary for the further averaging of data into a smaller number of spectra with a better S/N ratio. A preview of the data and of the associated reference, which includes derivative signals, can be done in order to define the extraction grid energy, but also to determine if an angular offset is necessary to apply on the data before starting the extraction. This option is very convenient, as an example if the monochromator was badly calibrated before starting the experiment (for instance a few tens of electron-volts). Indeed, considering the absorption spectrum of the known standard reference and assigning a known spectral feature to its tabulated values, the energy scale can be corrected according to the Bragg law relation, which relates the energy of the monochromatic beam to the angle of incidence in the crystal defined by its d-spacing. In that case, the same angular offset is applied to the data set contained in the folder under extraction.

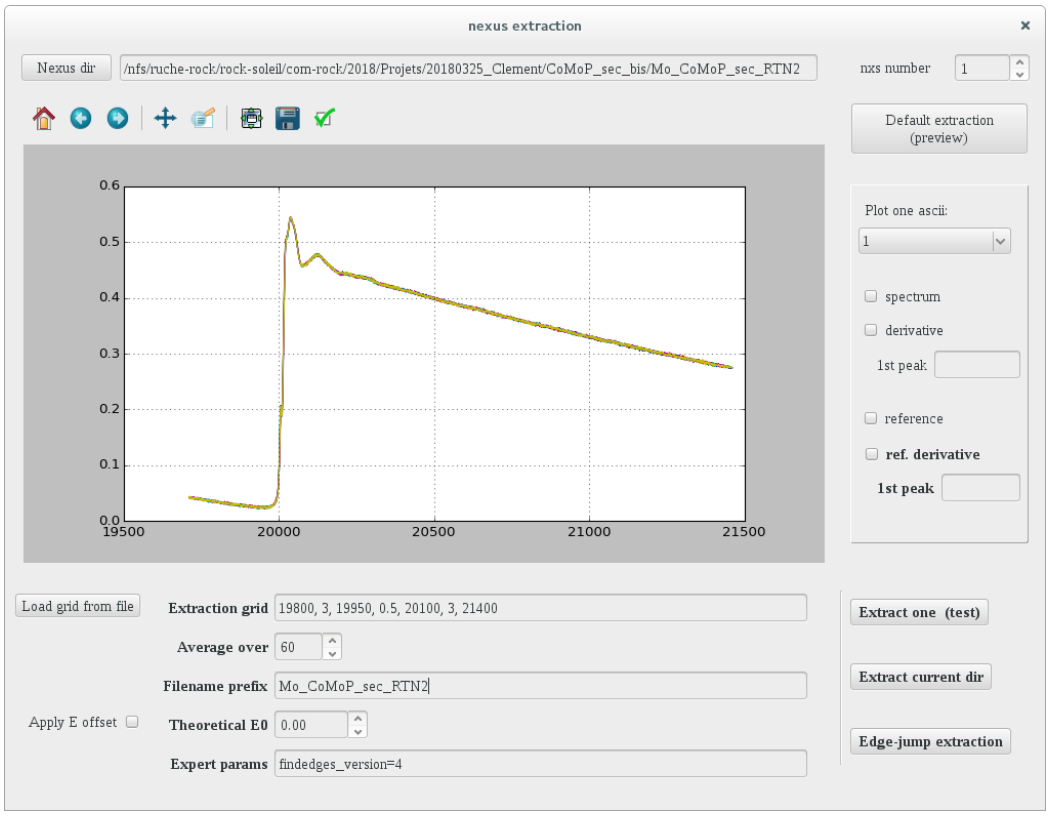

Figure S2 Extract_gui graphical user interface

The second graphical user interface, called *normal_gui* (Figure S3), processes the ASCII files created by *extract_gui* into calibrated and normalized data suitable to be used further as input files for MCR-ALS analysis.

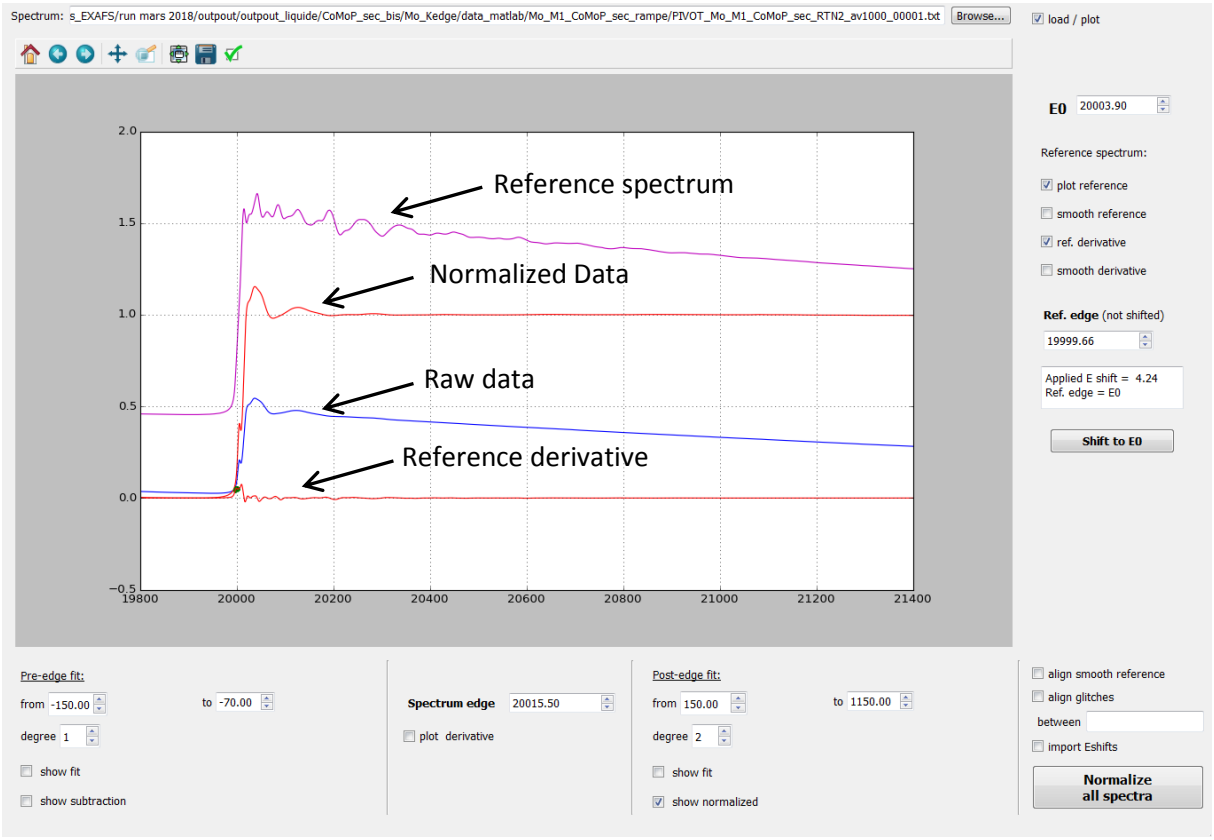

Figure S3 Normal_gui graphical user interface. Blue line is the raw spectrum and the red line is the normalized spectrum

Several options can be used for the ***energy calibration*** depending on the S/N ratio of the reference data or the experiment which has been carried out. Those options are defined on the right column of the GUI. In most cases, for transmission experiments, where a reference foil can be recorded at the same time than the data of interest with a satisfactory S/N ratio, the calibration is carried out on this reference by offsetting in energy the position of a known spectral feature to the tabulated one. A fit of the reference first derivate position (value in **Ref. edge** box) is done in order to help the user for the determination of its value. The user writes in the **E0** box the tabulated value and makes effective the shift of the energy scale by clicking the **Shift to E0** button.

For experiments where too noisy references are collected, smoothed derivatives of the reference can be used for energy calibration (option: align smooth reference). Finally when no reference is available, as it can happen for fluorescence experiments, energy calibration can be done on a selected glitch present in the energy range of the data and recorded on the first ionization chambers (option: align glitches).

The data ***normalization*** is carried out using the options in the bottom of the window. It deals with i) the removal of a linear function in the pre-edge region defined between two relative energy values (with respect to spectrum energy edge) defined in the energy range before the edge and ii) the calculation of a polynomial function (1^{st} or 2^{nd} order) in the post-edge range also defined by two user selected relative energy values. This post-edge polynomial function serves as atomic absorption function ($\mu_0(E)$) for evaluating the edge step with the extrapolation of the value of $\mu_0(E)$ to the spectrum energy edge. The edge jump so-calculated is used as a normalization factor to get the normalized absorption spectrum necessary to get rid of intensity variations associated to absorber concentration in the sample and any other aspects of measurements.

The determination of the normalization parameters on a selected spectrum (also called pivot spectrum) belonging to the data set of interest is done by visual inspection of the different steps of the calculation by checking the corresponding buttons ("show fits", "show subtraction" and "show normalized"). When those parameters are satisfactory, clicking on the **Normalize all spectra** button allows to perform calculations on each spectrum belonging to the data set using the same normalization parameters and imposing that the calibration strategy used for the pivot spectrum is also applied to each spectrum of the data set.

Both *extract_gui* and *normal_gui* belong to the extranormal software which is licensed under the GNU General Public License. This software has been developed under the Python programming language. The *normal_gui* interface is available on demand for the ROCK's users on windows and unix platforms.

5. XAS data processing

The background removal parameters for the EXAFS extraction are: E_0 = 20016 eV, pre-edge: -150 to -70 eV, post edge: 150 to 1150 eV, k-weight of 3 and spline range: 0 to 16.3 $Å^{-1}$ at the Mo K edge and E_0= 7713.5 eV, pre edge: -150 to -30 eV, post edge: 40 to 505 eV, k-weight of 2 and spline range: 0 to 12 $Å^{-1}$ at the Co K edge. The parameters of the Fourier Transform are dk =2, with a Kaiser-Bessel window, k-ranges are presented in Table 1.

Table 1 k range applied for each spectrum

Liquid Sulfidation		**Gas Sulfidation**	
Spectra	**k range ($Å^{-1}$)**	**Spectra**	**k range ($Å^{-1}$)**
L-MoO_aS_b	**2.7 -12.2**	G-MoO_aS_b	**2.9 – 12.8**
L-MoS_x	**1.7 – 10.8**	G-MoS_3	**1.8 – 11.5**
L-MoS_2	**1.8 – 12.1**	G-MoS_2	**1.7 – 12.1**
L-Co-C1	**2.4 – 8.3**	G-Co-C1	**2.4 – 10.5**
L-Co-C2	**2.4 – 8.8**	G-Co-C2	**2.0 – 10.1**
L-Co-C3	**2.0 – 9.5**	G-Co-C3	**2.0 – 10.3**

6. Fitting Results

Table 2 Least-squares fitting results of the EXAFS spectra of the Mo oxysulfide-like and sulfide MCR-ALS components obtained during liquid sulfidation (S_0^2=0.96, E_0=20016 eV)

Species	Contributions	R (Å) (±)	N (±)	σ^2 ($\times10^{-3}$ Å^2) (±)	$(\Delta\chi)^2$	N_{idp}	R-factor (%)	Enot (eV)
L-MoO_aS_b	Mo-O	1.64 (0.02)	1 (fixed)	9.8 (2.6)	4296	11	1.2	-1.55 (fixed)
	Mo-O	2.04 (0.01)	2 (fixed)	2.1 (0.8)				
	Mo-S	2.13 (0.01)	1 (fixed)	2.0 (1.0)				
	Mo-S	2.33 (0.01)	1 (fixed)	0.6 (1.0)				
	Mo-Al	2.61 (0.01)	1 (fixed)	2.1 (fixed)				
	Mo-Mo	2.65 (0.07)	1 (fixed)	22.1 (10.4)				
L-MoS_x	Mo-S	2.39 (0.01)	5.0 (0.8)	13.7 (2.6)	66267	12	1.9	-4.68
L-MoS_2	Mo-S	2.41 (0.04)	4.6 (0.1)	5.9 (0.3)	24069	11	0.8	-4.16
	Mo-Mo	3.19 (0.01)	1.4 (0.2)	5.8 (1.0)				

Table 3 Fitting results of the Co species obtained during liquid sulfidation (S_0^2=0.73, E_0=7713.5 eV)

Species	Contributions	R (Å) (±)	N (±)	σ^2 ($\times10^{-3}$ Å^2) (±)	$(\Delta\chi)^2$	N_{idp}	R-factor (%)	Enot (eV)
L-Co-C1	Co-O	2.06 (0.01)	6 (fixed)	6.3 (1.2)	462	4	0.2	5.75
L-Co-C2	Co-O	2.00 (0.01)	4.0 (0.5)	6.3 (fixed)	827	5	1.7	3.97
L-Co-C3	Co-S	2.22 (0.01)	4.0 (0.2)	7.4 (0.5)	279	8	0.2	3.69 (fixed)
	Co-Co	2.62 (0.02)	0.8 (0.3)					
	Co-Mo	2.74 (0.04)	0.7 (0.3)					

Table 4 EXAFS Fitting results of the Mo oxysulfide-like and sulfide MCR-ALS components obtained during gas sulfidation (S_0^2=0.96, E_0=20016 eV)

Species	Contributions	R (Å) (±)	N (±)	σ^2 ($\times10^{-3}$ Å^2) (±)	$(\Delta\chi)^2$	N_{idp}	R-factor (%)	Enot (eV)
G-MoO_aS_b	Mo-O	1.62 (0.01)	1 (fixed)	4.7 (1.0)	1057	11	0.4	-1.55 (fixed)
	Mo-O	2.01 (0.01)	2.5 (fixed)	7.7 (0.8)				
	Mo-S	2.42 (0.01)	2 (fixed)	8.0 (0.8)				
	Mo-Al	2.61 (0.02)	0.5 (fixed)	4.3 (3.5)				
	Mo-Mo	2.78 (0.04)	1 (fixed)	18.5 (6.9)				
G-MoS_3	Mo-S	2.38 (0.01)	4.1 (0.1)	8.9 (0.5)	6279	11	0.4	-6.47
	Mo-Mo	2.80 (0.02)	2.9 (0.7)	22.7 (3.9)				
G-MoS_2	Mo-S	2.41 (0.01)	4.9 (0.2)	5.5 (0.5)	11940	11	0.9	-4.74
	Mo-Mo	3.18 (0.01)	1.6 (0.4)	5.4 (1.7)				

Table 5 Fitting results of the Co species obtained during gas sulfidation (S_0^2=0.73, E_0=7713.5 eV)

Species	Contributions	R (Å) (±)	N (±)	σ^2 ($\times10^{-3}$ Å^2) (±)	$(\Delta\chi)^2$	N_{idp}	R-factor (%)	Enot (eV)
G-Co-C1	Co-O	2.06 (0.01)	6 (fixed)	6.6 (0.7)	2454	9	0.4	6.13
G-Co-C2	Co-S	2.25 (0.01)	5.5 (0.3)	5.4 (0.7)	2815	6	0.4	4.5
G-Co-C3	Co-S	2.23 (0.01)	3.9 (0.1)	7.3 (0.4)	864	10	0.2	4.40
	Co-Co	2.64 (0.03)	0.5 (0.2)					
	Co-Mo	2.74 (0.04)	0.4 (0.2)					

Table 6 Fitting results of the final MoS_2 species at room temperature after liquid and gas sulfidation (S_0^2=0.96, E_0=20016 eV, k ranges: 1.8 – 12.1 for both fits)

Species	Contributions	R (Å) (±)	N (±)	σ^2 ($\times 10^{-3}$ Å^2) (±)	$(\Delta\chi)^2$	N_{idp}	R-factor (%)	Enot (eV)
L-MoS_2 RT	Mo-S	2.41 (0.01)	4.4 (0.2)	2.8 (0.5)	32358	11	0.8	-3.16
	Mo-Mo	3.18 (0.01)	1.8 (0.3)	2.7 (1.1)				
G-MoS_2 RT	Mo-S	2.41 (0.01)	5.2 (0.3)	2.6 (0.5)	17921	11	0.9	-3.16
	Mo-Mo	3.18 (0.01)	2.7 (0.4)	2.7 (0.9)				

7. EXAFS information

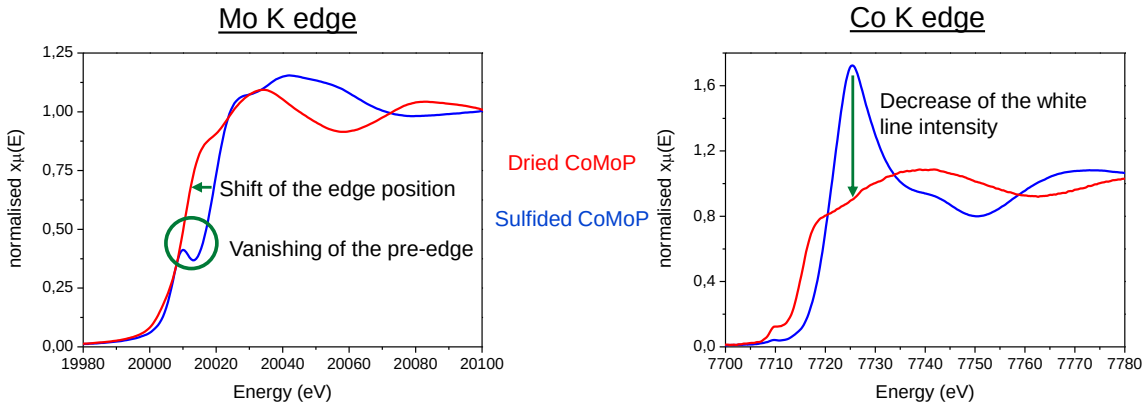

Figure S4 Highlight of the EXAFS key features indicating the sulfidation of a CoMoP catalyst at the Co and Mo K edge

8. Slope break in the evolution of the edge position

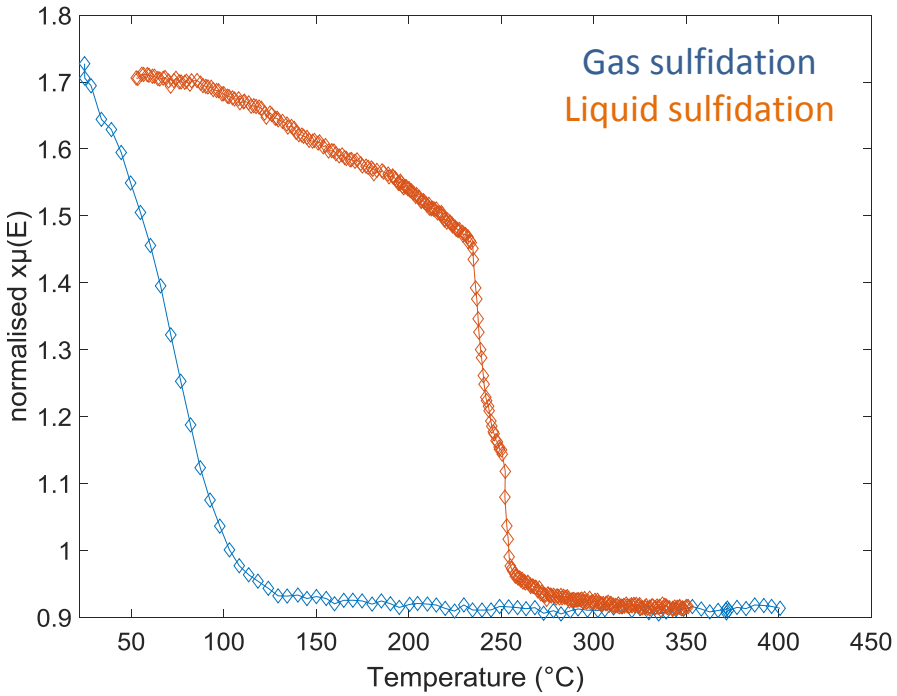

Figure S5 White line (7726 eV) evolutions at the Co K edge for the liquid (orange curve) and the gas (blue curve) sulfidation

9. Raman spectroscopy

- **Oxide Spectra**

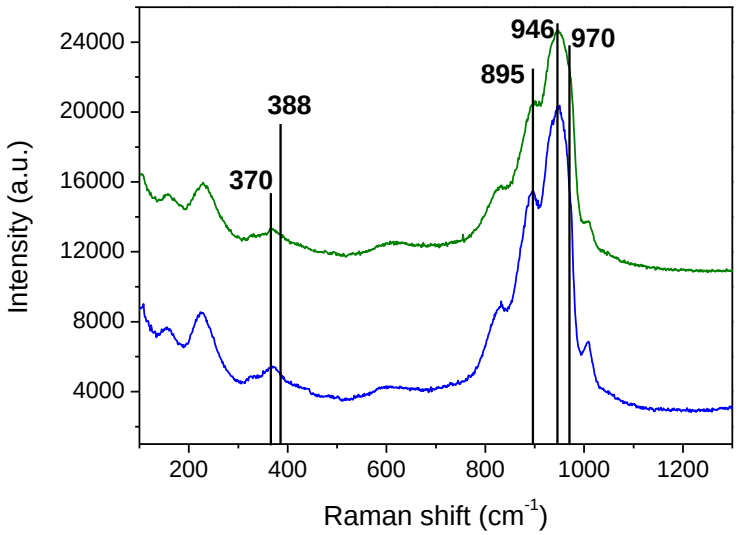

Figure S6 Raman Spectra of the dried CoMoP catalyst used in gas sulfidation (blue) and liquid sulfidation (green) from two different batches. Raman lines at 970 cm^{-1}, 946 cm^{-1}, 895, cm^{-1}, 388 cm^{-1} and 369 cm^{-1} evidence to the presence of Strandberg HPA ($H_xP_2Mo_5O_{23}^{6-x}$), Keggin HPA ($H_xPMo_{12}O_{40}^{3-x}$) and heptamolybdate ($H_xMo_7O_{24}^{6-x}$) [1,2]. Therefore, there is the same mixture of Strandberg, Keggin HPA and polymolybdates species on the catalysts used in gas and liquid sulfidation.

- **Operando Raman spectra**

The obtained Raman spectra are normalised on the N_2 peak at 2329 cm^{-1}. Only spectra of the gas phase (Figure S7) are used to follow the evolutions of CH_4 and H_2S. They are determined by the evolution of the peak maximum intensity at 2612 cm^{-1} for H_2S and 2918 cm^{-1} for CH_4. The gas phase spectra still contain gas oil signal between 2800 cm^{-1} and 3000 cm^{-1} which has been subtracted using pure gas oil signal. The cleaned up gas spectra are presented in Figure S8 and the evolution of H_2S and CH_4 is presented in Figure S9.

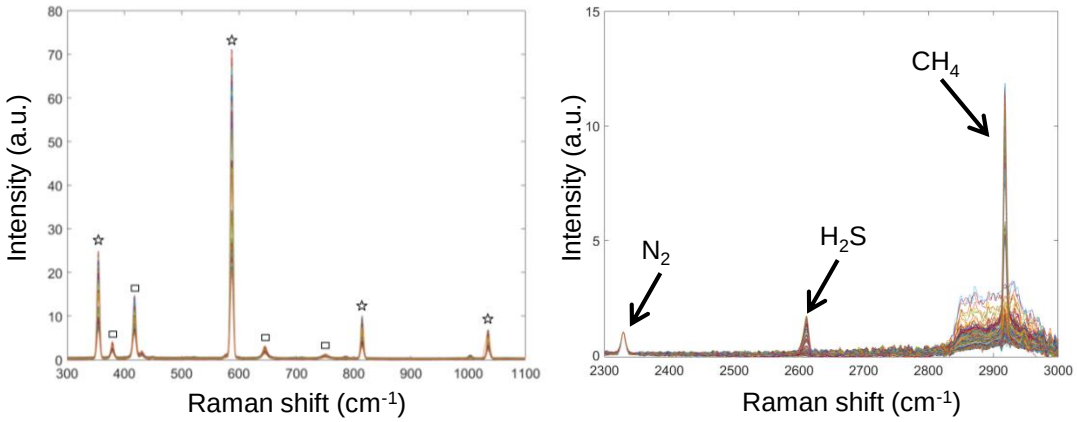

Figure S7 Raman Spectra of the gas phase recorded at the cell outlet during the liquid sulfidation of the dried CoMoP catalyst (☆: H_2 peaks, ▭ : Sapphire peak)

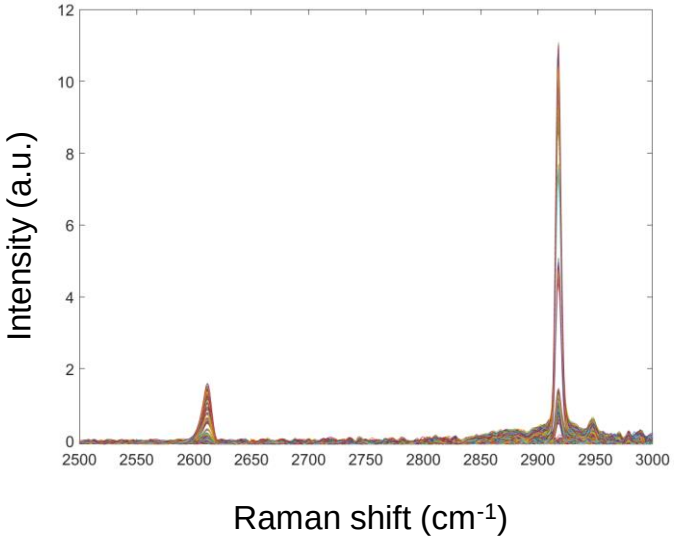

Figure S8 Raman spectra of the gas phase after removal of the gas oil signal

Figure S9 displays the evolution of the peak intensity for H_2S (at 2612 cm^{-1}) and CH_4 (at 2918 cm^{-1}). The decomposition of DMDS is characterised by the detection of CH_4 at 226±5°C which is in agreement with the work of Texier *et al.* [3]. H_2S is detected at 274±5°C. The gap of 48°C is assigned to the consumption of H_2S by the catalyst during the liquid sulfidation.

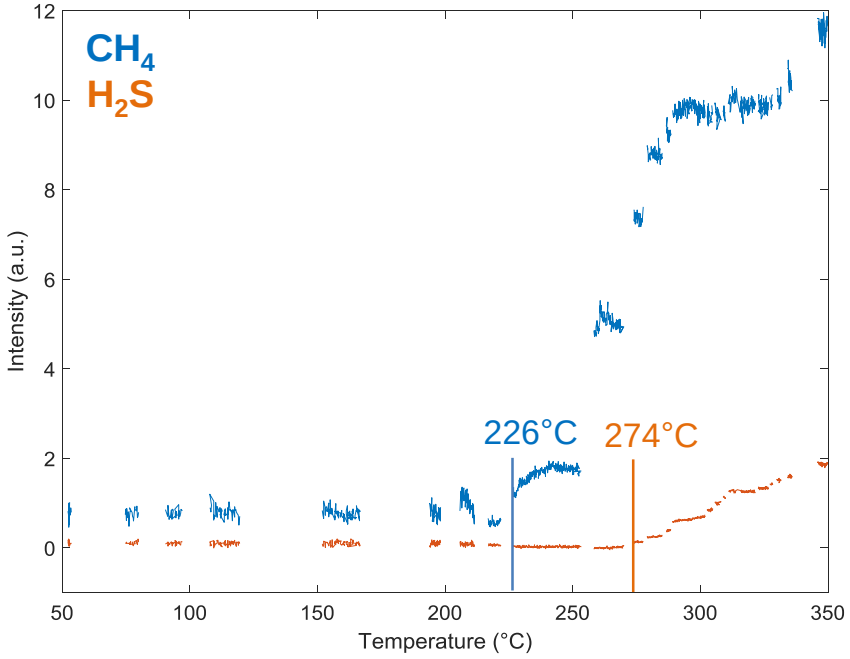

Figure S9 Evolution of the intensity maximum of the Raman lines characteristic of gaseous H_2S and CH_4.

10. Gas sulfidation with a supply of H_2S at 210°C

The same gas sulfidation as described in section 2.2.4 was performed with 2 modifications:

- for beamtime issues, the heating rate was increased at 180°C.h^{-1}
- From 20°C till 210 °C, the feed was composed of pure H_2 and between 210°C and 350°C, a feed of 15v% H_2S/H_2 was used

Figure S10 represent the concentration evolution of the Co species during this specific gas sulfidation and their XANES spectra. Table 7 shows fitting results of the Co species obtained during the gas sulfidation. Figure S10 and Table 7 evidence a similar behaviour of Co species as in the liquid sulfidation, i.e. a shortening of first coordination shell distance, a decrease of coordination numbers from 6 to 4, together with a slight increase of the pre-edge feature in the Co K edge XANES data.

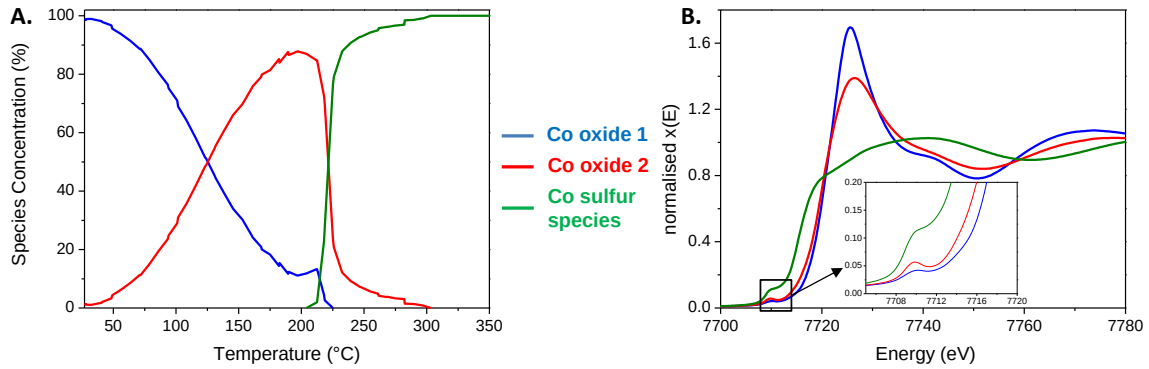

Figure S10 Concentration profile (A.) of a dried CoMoP catalyst at the Co K edge during a gas sulfidation with an H_2S supply at 210 °C and XANES spectra of the EXAFS spectra associated to the MCR-ALS components determined from the analysis of the data recorded at the Co K edge (B.)

Table 7 Fitting results of the Co species obtained during the liquid sulfidation (S_0^2=0.73, E_0=7713.5 eV, Pre edge: -150 to -30 eV, post edge: 40 to 505 eV, k-weight of 2 and spline range: 0 to 12 Å^{-1}, k ranges: 2.4 – 10.2 (Co oxide 1) and 2.7 – 9.8 (Co oxide 2)

Species	Contributions	R (Å) (±)	N (±)	σ^2 (Å^2×10^3) (±)	$(\Delta\chi)^2$	N_{idp}	R-factor (%)	Enot (eV)
Co oxide 1	Co-O	2.07 (0.01)	6 (fixed)	6.4 (1.1)	3627	7	0.1	6.65
Co oxide 2	Co-O	1.99 (0.02)	4.1 (0.3)	6.4 (fixed)	1271	7	0.1	3.17

11. PCA and MCR-ALS results

XAS Mo K edge data of the CoMoP catalyst during the liquid sulfidation

PCA and MCR-ALS were used to identify the intermediate species and their concentration profiles in the experimental XAS data. These methods are based on the bilinearity form of the experimental data set D expressed under a matrix form. The matrix D ($m_{\times}n$) containing the experimental data is arranged so that each vertical column has variables, herein the energy of the monochromator, and, each horizontal row contains samples, herein the absorbance of one spectrum. Principal components decomposed the experimental matrix into the product of two matrices, the score matrix (T) and the loading matrix (L). This transformation is orthogonal and linear. In addition, the loadings are defined as orthogonal vectors. Thus, **D=T.L**.

The use of Singular Value Decomposition (SVD) algorithm allows the calculation of the Principal Components (PC) of D. In that case, the D matrix is factorized in the following equation: $\mathbf{D=U.S.V^T}$. U and V^T are unitary orthogonal matrices with a respective size of $m_{\times}m$ and $n_{\times}n$ and S is a diagonal matrix ($m_{\times}n$) with non-negative real numbers called eigenvalues. The score matrix (T) is equal to the product of U.S and the loading matrix (L) is equal to V^T.

To determine the number of PCs which describes the maximum of variance of the experimental data, two main graphical representations are used:

- Log-scale scree plot
- The representation of the elements for the U matrix of each PC as a function of the number of spectra.

The log-scale scree plot represents the PC eigenvalues sorted out a function of their importance regarding to the variance that they can explain in the whole dataset (the variance being defined as the square of the eigenvalue). For sake of clarity the log-scale scree plot is herein displayed for the first 20 PC. The required number of PCs is ascribed to the slope break between the straight line formed by the first PCs and a second asymptotic line which aim to pass through the other dots corresponding to components of lower eigenvalues with no contribution to explain system variance. Herein, in Figure S11, the experimental data at the Mo K edge of the CoMoP catalyst during the liquid sulfidation could be described by 4 or 5 principal components.

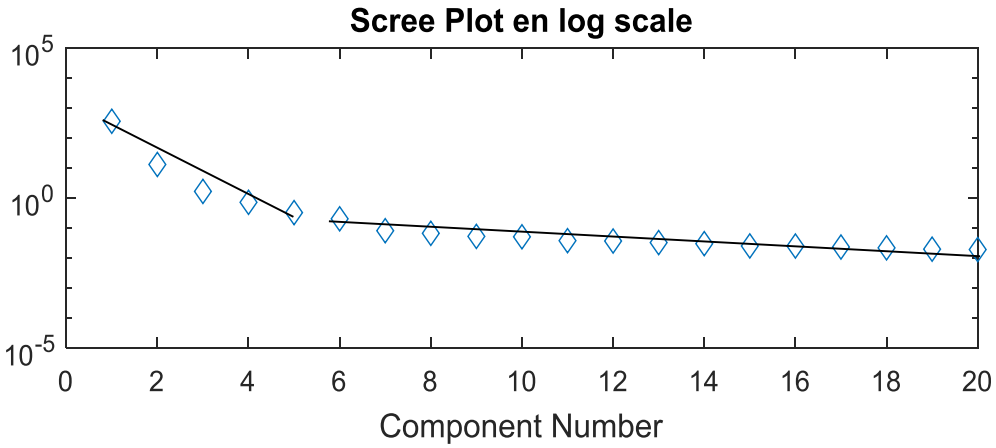

Figure S11 Log-scale scree plot of the CoMoP catalyst at the Mo K edge during the liquid sulfidation

The representation of the elements for the U matrix for the first PCs as a function of the number of spectra in D is presented in Figure S12 It deals with the plot of the u_{ij} elements with i and j varying

from 1 to m, m being the number of spectra. During the monitoring of a kinetic, spectra are assumed to be ordered according to a variable (time, temperature, pH, etc...). Thence, trajectories are expected for the PCs which are significant. From PCA 1 to PCA 5, clear trajectories are seen, whereas the PCA 6 seems to contain some noise. This representation indicates the presence of 5 PCs to describe the system. If there is a doubt about the number of PCs, the minimization by MCR-ALS is performed with the N number of PCs, N+1 and N-1. Then, the results of the 3 simulations are compared with each other and with additional data to find the meaningful simulations. As an example, obtained spectra could be fitted and the results compared to the literature to see if they are relevant chemical compounds. The concentration profiles may be compared with online data such as the H2S and CH4 release to see common features. Therefore, the best minimization should be converging and chemically relevant with the chemical knowledge available. Combining the results of the scree plot and this so-called scores trajectory representation, it is concluded that 5 PC are required to describe the liquid sulfidation of the CoMoP catalyst at the Mo K edge.

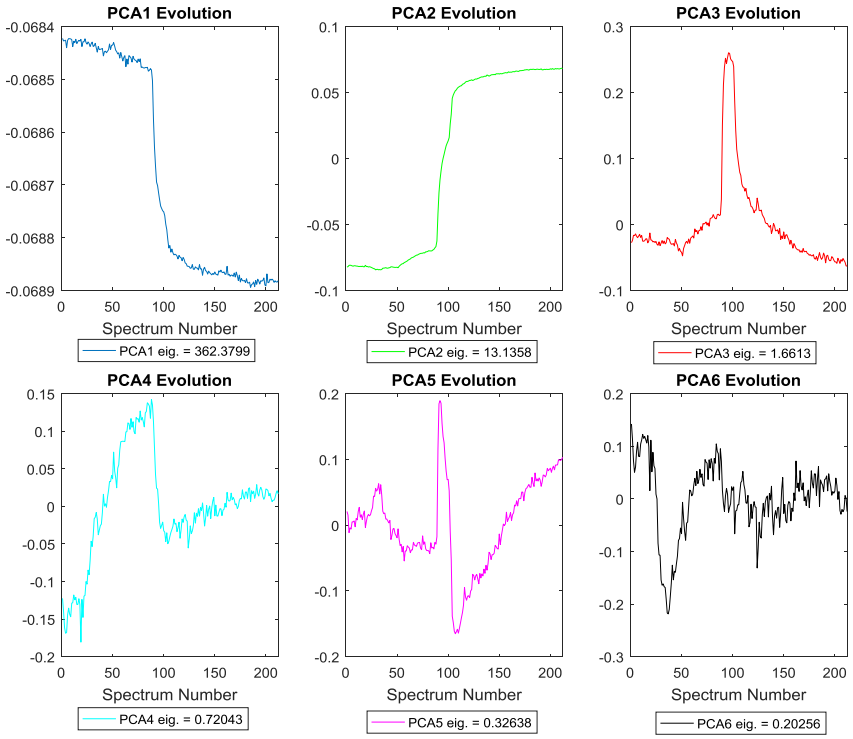

Figure S12 Representation of the elements for the U matrix of each PC as a function of the number of spectra of the CoMoP catalyst during the liquid sulfidation at the Mo K edge

The required number of PC to explain the variance of system is then used as input for the rank of matrices C and S in the MCR-ALS minimization. This method allows the isolation of intermediates without the use of reference spectra. Indeed, in heterogeneous catalysis, the use of reference spectra in least square fitting linear combination has been shown often inappropriate due to different recording conditions compared to the samples or due to different crystallinity and/or dispersion [4].The D matrix is decomposed by the following equation: $\mathbf{D=C.S^T+E}$, C matrix contains the concentration profiles of the pure components, S^T is the transposed matrix of S which is composed of the normalized XAS spectra of the pure components and E the experimental uncertainties. The equation is solved mathematically by iteration and least square minimization of the E matrix. Constraints on the C and S matrices may be applied to obtain chemically and physically meaningful results. In this work 3 constraints were used for the C matrix:

- Non negativity of the concentration
- Unimodality: each species concentration reaches only one maximum
- Closure relation: at any time the sum of the concentration profiles is equal to 100%

For the S matrix, only a non-negativity constraint was applied on the absorbance of the normalized spectra.

The evolving factor analysis (EFA) algorithm is used in order to build a first guess of the C matrix [5]. It is based on an iterative calculation of the singular values of submatrices of the data matrix. There are two steps, a first one in the forward direction which allows the appearance of the species to be determined along the reaction coordinates and a second one in the backward direction to describe the disappearance of chemical species. Starting from this estimation, a first concentration profile is set to be used in the first iteration of the least square minimization. The MCR-ALS program (MCR-ALS GUI 2.0) was developed by Roma Tauler and his group on the Matlab® platform [6].

Figure S13 presents the results of the MCR-ALS minimisation on the Mo K edge normalised XAS data of the CoMoP catalyst during its liquid sulfidation. Convergence was achieved after 15 iterations leading to the alternate minimization of C and S.

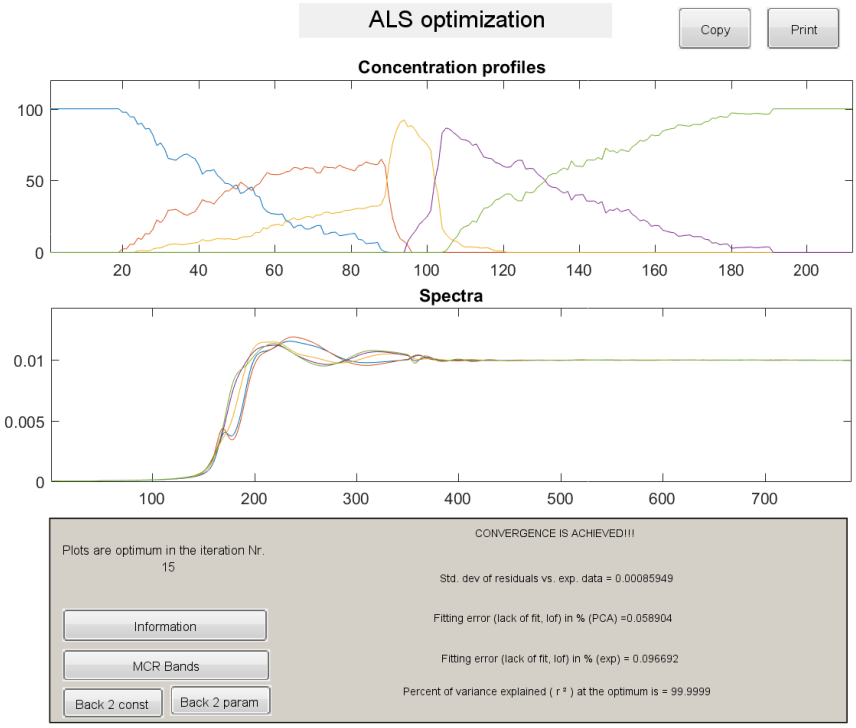

Figure S13 Results of the MCR-ALS minimisation on the Mo K edge normalised XAS data of the CoMoP catalyst during its liquid sulfidation.

The obtained normalised spectra are, then, fitted with Artemis program. Figure S14 presents the FT of the oxysulfide, MoS_x and MoS_2 and their respective fits. The results of these fits are shown in Table 2.

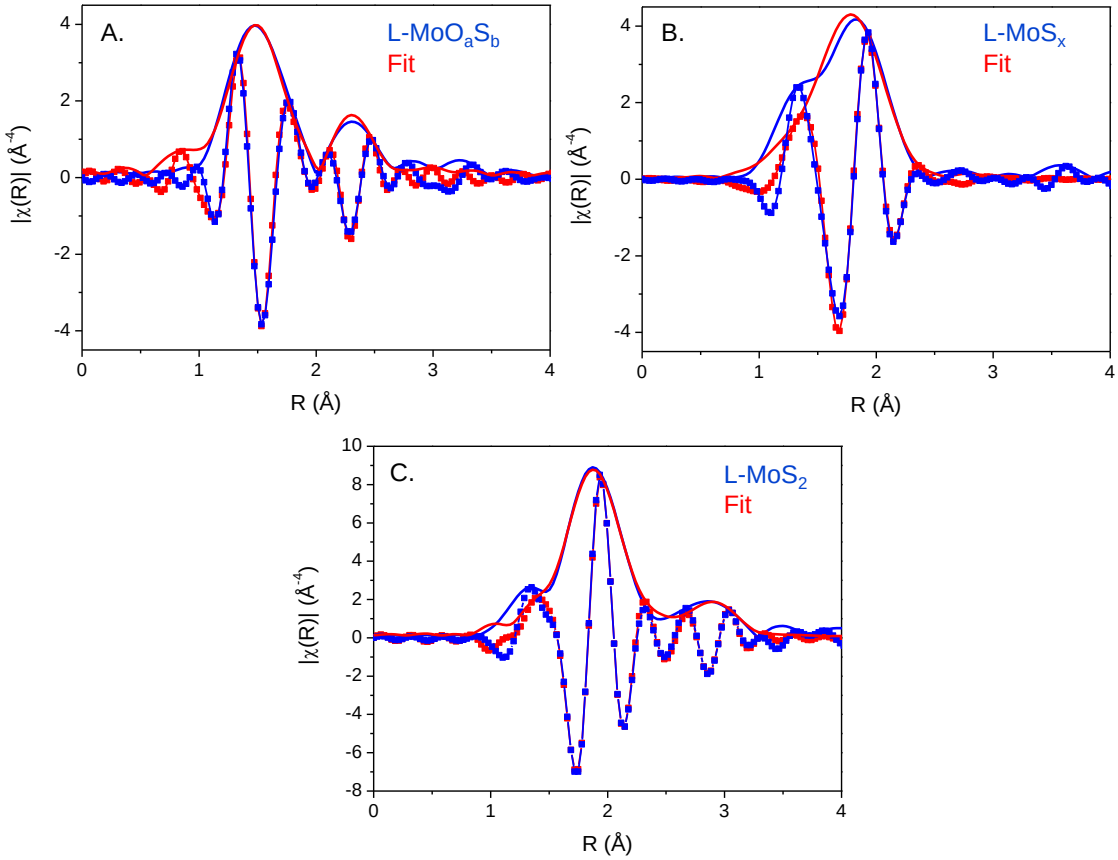

Figure S14 FT of the XAS spectra of the L-MoO$_a$S$_b$ (A.), MoS$_x$ (B.) and MoS$_2$ (C.) and their respective fits. Magnitude is represented in lines and the imaginary part in dots connected with lines

The same procedure was applied to the data at the Co K edge of the liquid sulfidation and for both edges of the gas sulfidation.

Liquid sulfidation: Co K edge

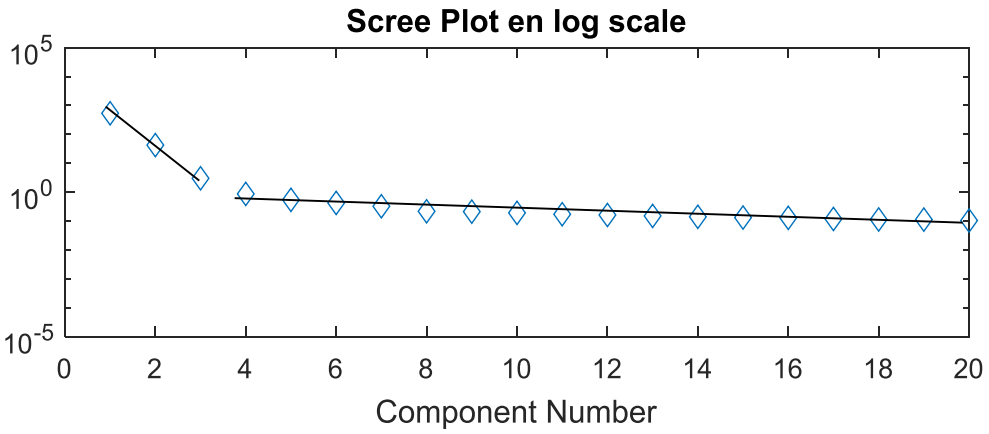

Figure S15 Log-scale scree plot of the CoMoP catalyst at the Co K edge during the liquid sulfidation. The slope break occurs at 3 PC.

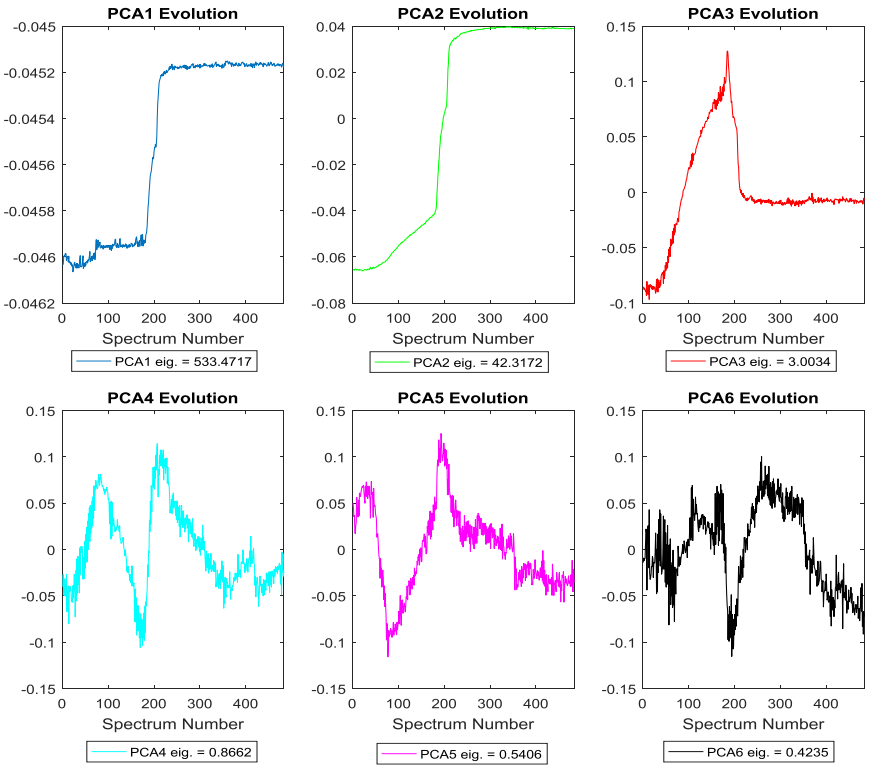

Figure S16 Representation of the elements for the U matrix of each PC as a function of the number of spectra of the CoMoP catalyst during the liquid sulfidation at the Co K edge

3 PCs are required for the MCR-ALS minimization of the recorded data set at the Co K edge during liquid sulfidation.

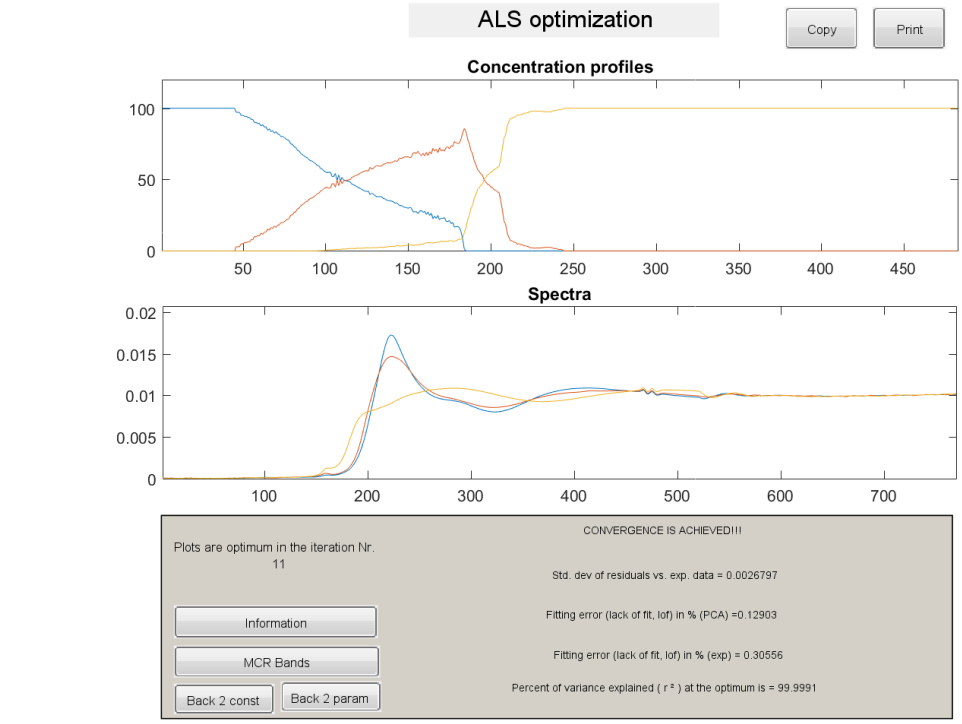

Figure S17 Results of the MCR-ALS minimisation on the Co K edge normalised XAS data of the CoMoP catalyst during its liquid sulfidation.

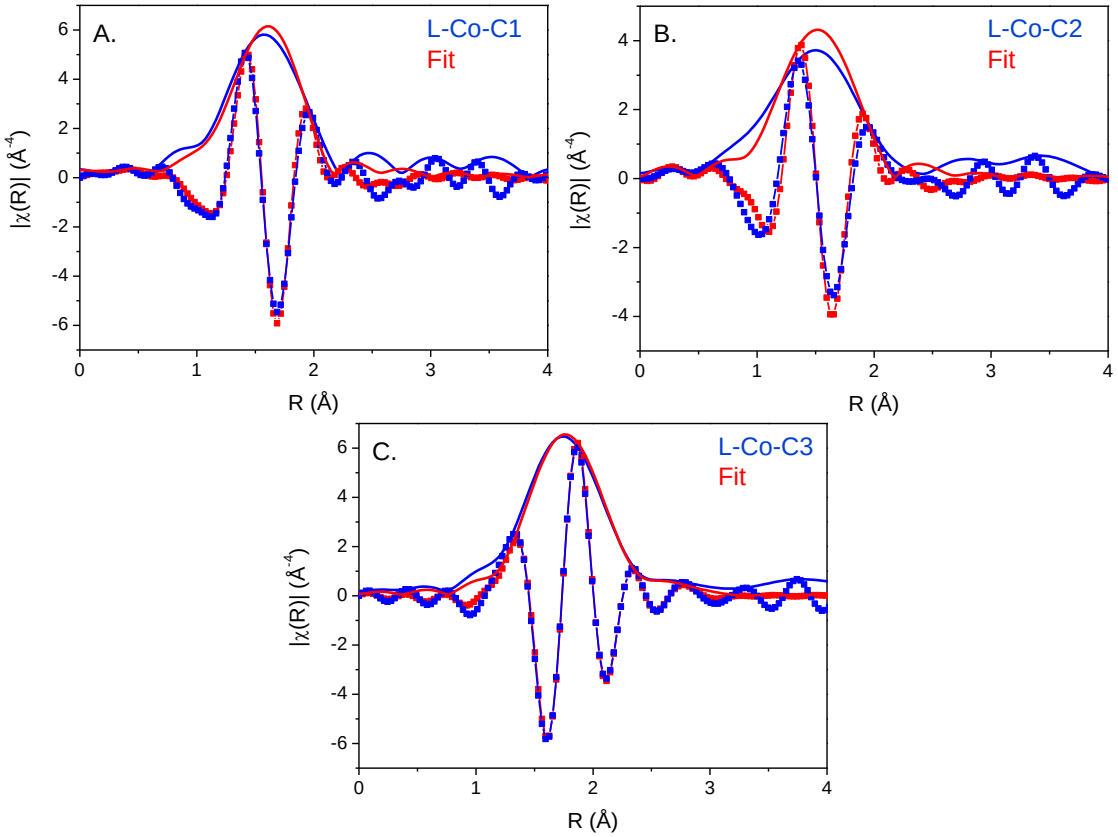

Figure S18 FT of the XAS spectra of the L-Co-C1 (A.), L-Co-C2 (B.) and L-Co-C3 (C.) and their respective fits. Fitting results are presented in Table 3.

Gas Sulfidation: Mo K edge

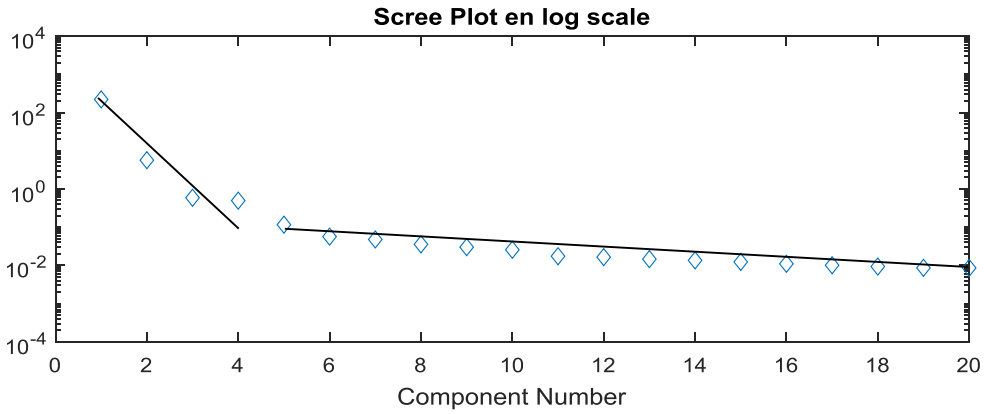

Figure S19 Log-scale scree plot of the CoMoP catalyst at the Mo K edge during the gas sulfidation. The slope break occurs at 4 PCs.

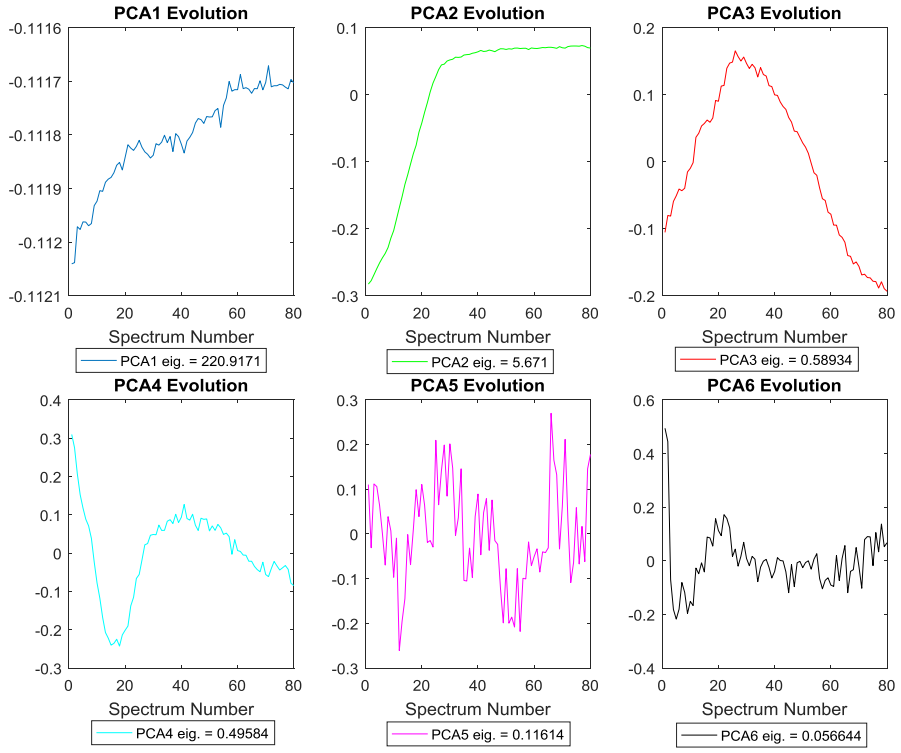

Figure S20 Representation of the elements for the U matrix of each PC as a function of the number of spectra of the CoMoP catalyst during the gas sulfidation at the Mo K edge

4 PCs are required for the MCR-ALS minimization of the Mo K edge data set recorded during the gas sulfidation.

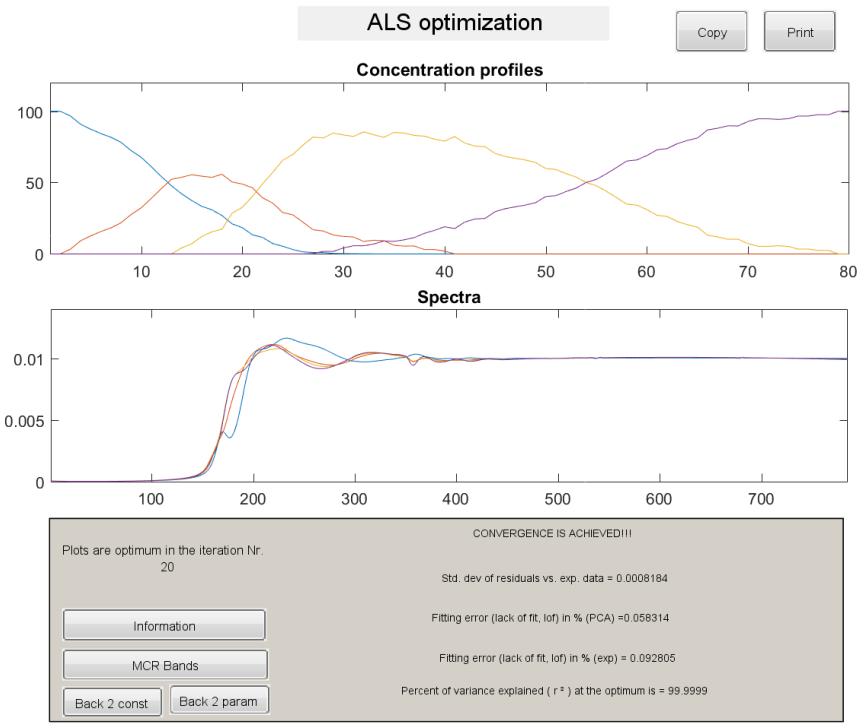

Figure S21 Results of the MCR-ALS minimisation on the Mo K edge normalised XAS data of the CoMoP catalyst during its gas sulfidation.

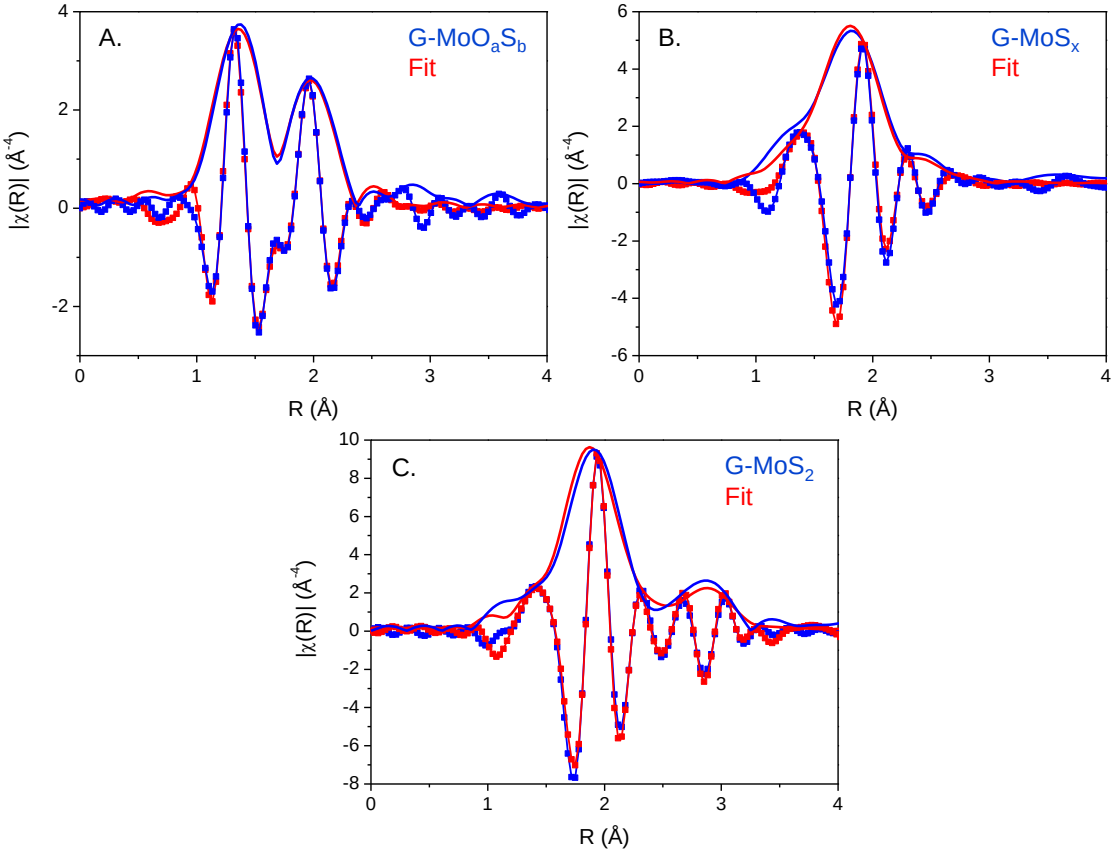

Figure S22 FT of the XAS spectra of the L-Co-C1 (A.), L-Co-C2 (B.) and L-Co-C3 (C.) and their respective fits. Fitting results are presented in Table 4.

Gas sulfidation: Co K edge

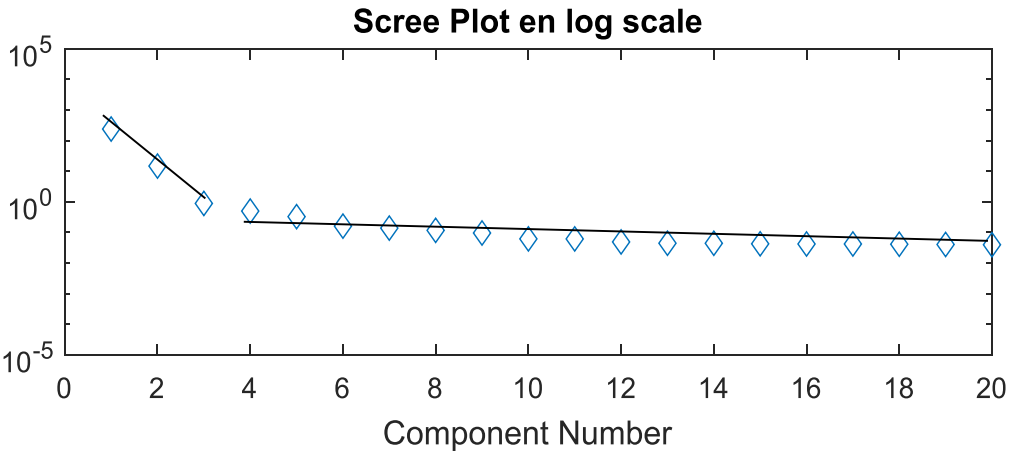

Figure S23 Log-scale scree plot of the CoMoP catalyst at the Mo K edge during the gas sulfidation. The slope break occurs at 3 PCs.

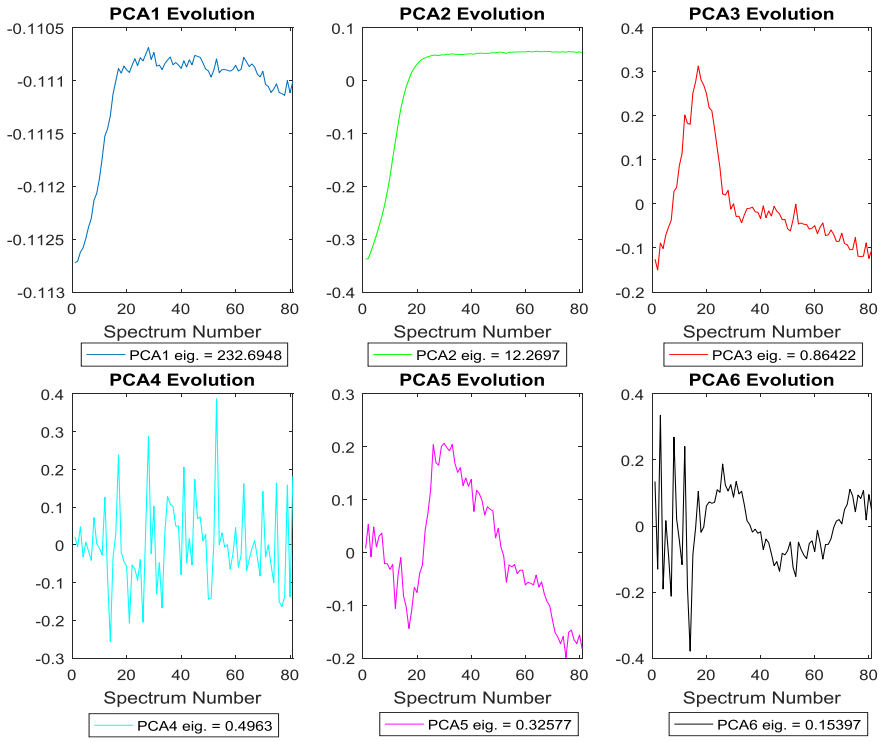

Figure S24 Representation of the elements for the U matrix of each PC as a function of the number of spectra of the CoMoP catalyst during the gas sulfidation at the Co K edge

3 PCs are required for the MCR-ALS minimization of the Co K edge data set recorded during the gas sulfidation.

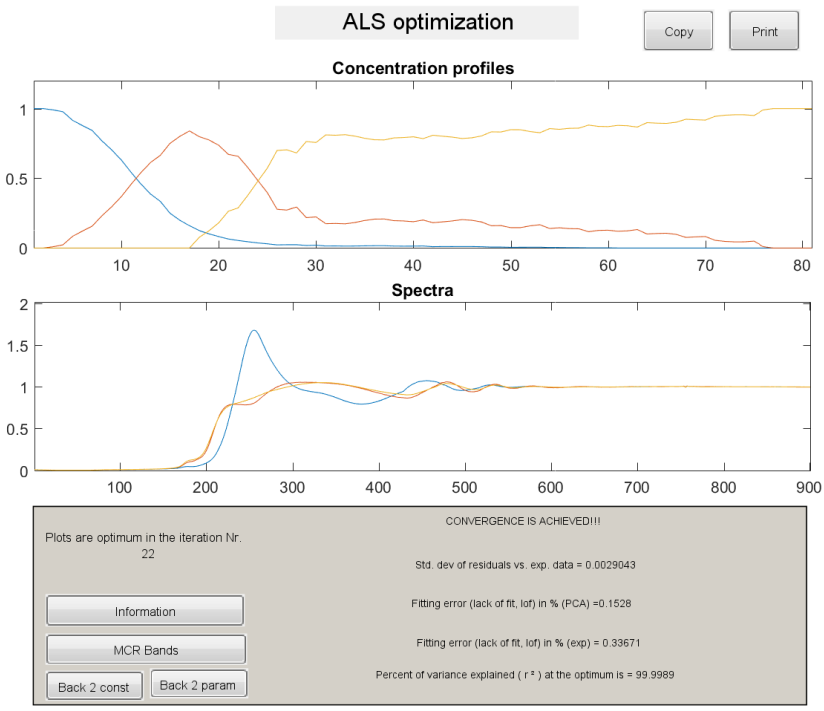

Figure S25 Results of the MCR-ALS minimisation on the Co K edge normalised XAS data of the CoMoP catalyst during its gas sulfidation.

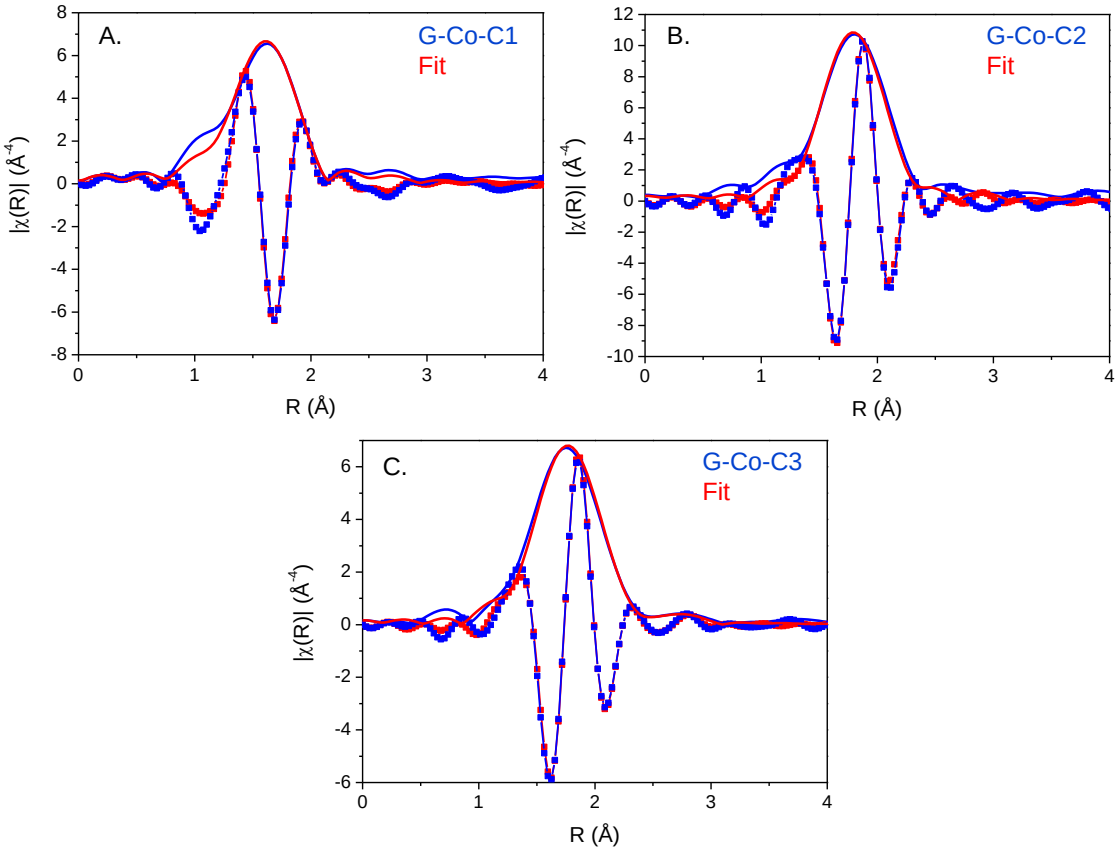

Figure S26 FT of the XAS spectra of the G-Co-C1 (A.), G-Co-C2 (B.) and G-Co-C3 (C.) and their respective fits. Fitting results are presented in Table 5.

12. Comparison of the oxysulfide and the MoS_x species isolated by MCR-ALS in gas and liquid phase

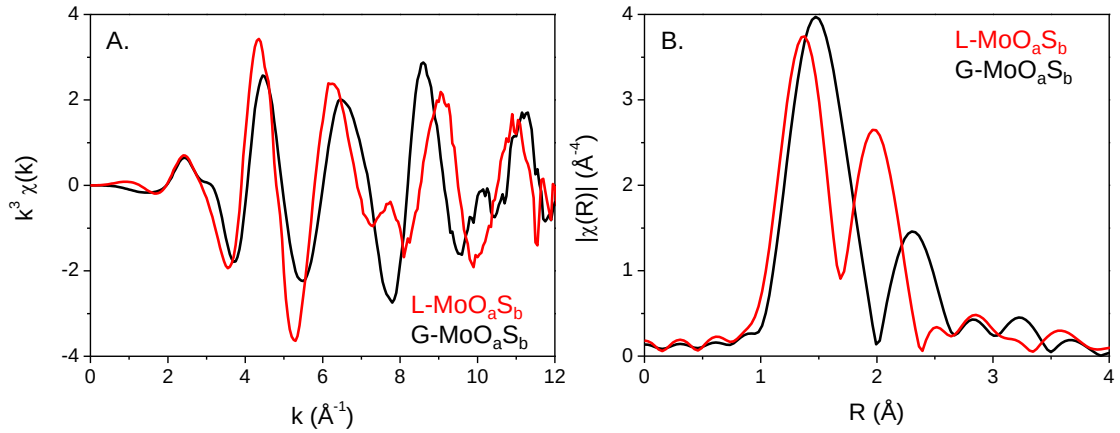

Figure S27 EXAFS spectra (A.) and Fourier transforms (B.) of the MoO_aS_b species identified in liquid and gas sulfidation at the Mo K edge.

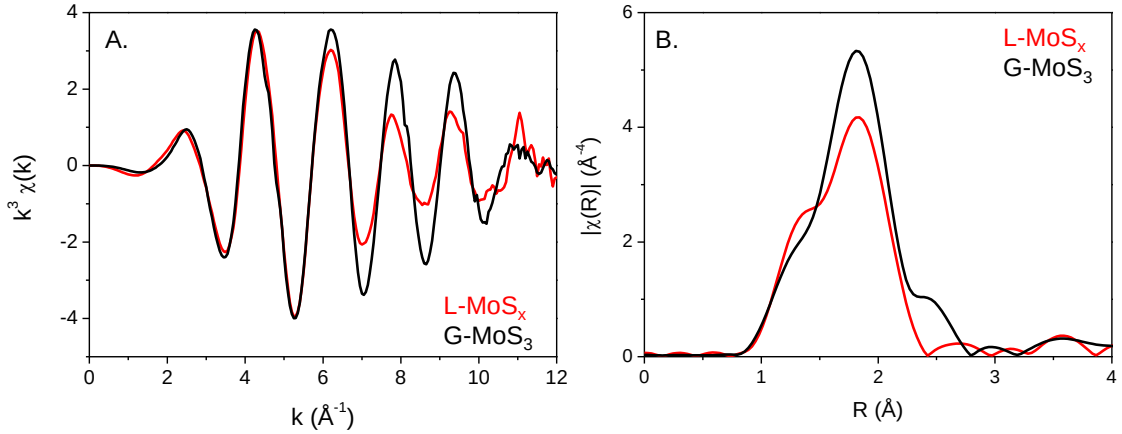

Figure S28 EXAFS spectra (A.) and Fourier transforms (B.) of the L-MoS_x and G-MoS_3 identified in liquid and gas sulfidation at the Mo K edge.

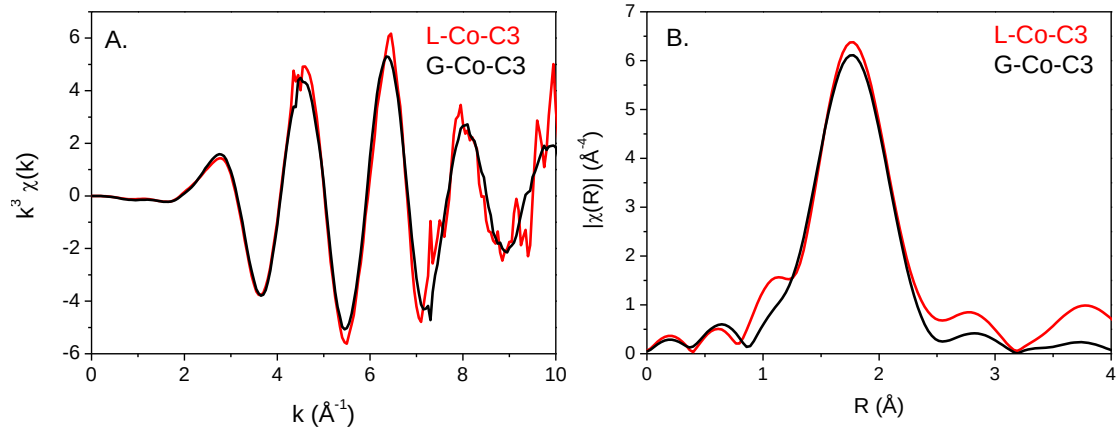

Figure S29 EXAFS spectra (A.) and Fourier transforms (B.) of the Co-C3 species identified in liquid and gas sulfidation at the Co K edge

13. TEM results

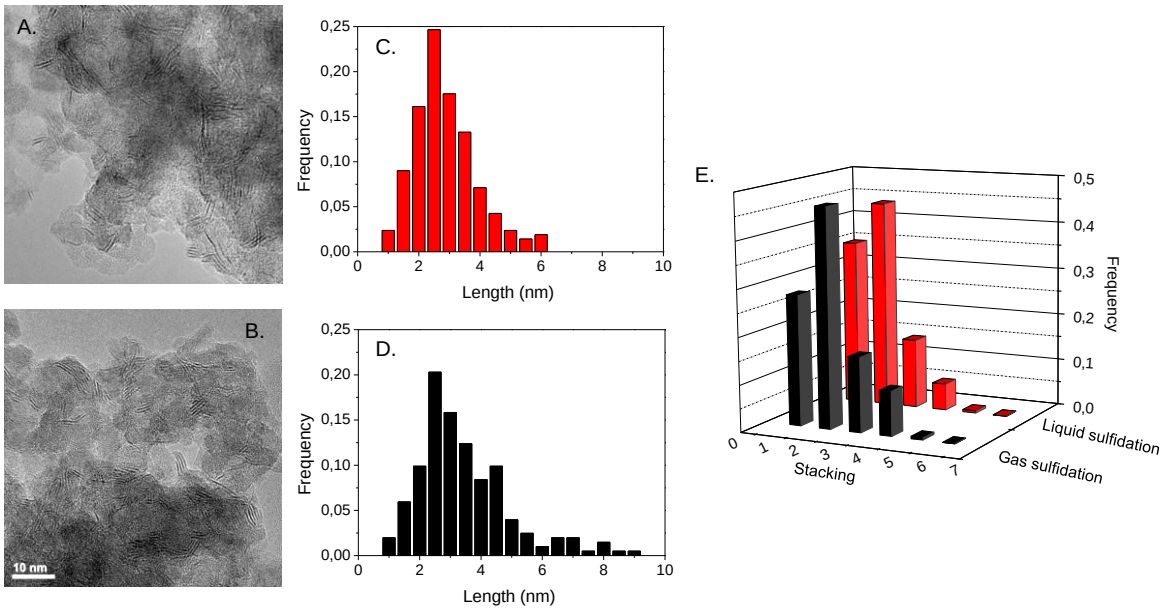

Figure S30 TEM pictures (liquid sulfidation (A.) and gas sulfidation (B.)), slab length histogram (C. and D.) and stacking histogram (E.) of the sulfided CoMoP catalyst under liquid (red) and gas (black) sulfidation.

Table 7 Average length and stacking of a dried CoMoP catalyst sulfided with either liquid sulfidation or gas sulfidation

Sulfidation	Average Length (Standard deviation)	Average Stacking (Standard deviation)
Liquid	2.9 (1.0)	1.9 (0.9)
Gas	3.5 (1.7)	2.1 (0.9)

References

[1] L. Catita, A.-A. Quoineaud, D. Espinat, C. Pichon, O. Delpoux, Appl. Catal. A Gen. 547 (2017) 164–175.

[2] P. Blanchard, C. Lamonier, A. Griboval, E. Payen, Applied Catalysis A: General 322 (2007) 33–45.

[3] S. Texier, G. Berhault, G. Pérot, V. Harlé, F. Diehl, J. Catal. 223 (2004) 404–418.

[4] W.H. Cassinelli, L. Martins, A.R. Passos, S.H. Pulcinelli, C.V. Santilli, A. Rochet, V. Briois, Catal. Today 229 (2014) 114–122.

[5] M. Maeder, Anal. Chem. 59 (1987) 527–530.

[6] J. Jaumot, A. de Juan, R. Tauler, Chemom. Intell. Lab. Syst. (2015) 1–12.